**CHARACTERIZATION OF THE LUNAR SURFACE WITHIN TSIOLKOVSKY CRATER: THE PHOTOMETRIC, ALBEDO, AND THERMAL PROPERTIES OF THE REGOLITH.** D. L. Domingue,[1] E. E. Palmer,[1] R. Gaskell,[1] M. Staid[1], and C. M. Pieters[2], [1](domingue@psi.edu) Planetary Science Institute 1700 E. Fort Lowell, Suite 106, Tucson AZ, 85719, USA. [2]Brown University, Providence RI, 02912, USA.

**Introduction:** After suspecting hydrated materials might exist on the Moon [1], the actual detection of surficial $OH/H_2O$ on the Moon by 4 different missions has changed our views of the interactions of the lunar surface with the space environment and the stability of water on its surface [2-5]. Most results stem from examination of spectra beyond 2μm, where reflected sunlight and thermal emission both contribute to the spectral signature. The detection and examination of the $OH/H_2O$ signatures across the surface are dependent on the removal of the thermal signature, which is especially difficult for the Moon Mineralogy Mapper ($M^3$) data [2].

Photometric characterization of a surface can provide information on the physical structure of a surface (such as roughness) in addition to derivation of surface albedo properties (geometric and Bond albedos). This characterization is highly dependent on the accuracy to which the illumination and viewing conditions can be determined. We present a technique that allows us to utilize local topographic information (on meter scales) to photometrically characterize the lunar surface, and provide the albedo information needed to generate a thermal correction for the $M^3$ data, improving the dectection and mapping the distribution of $OH/H_2O$ across the lunar surface.

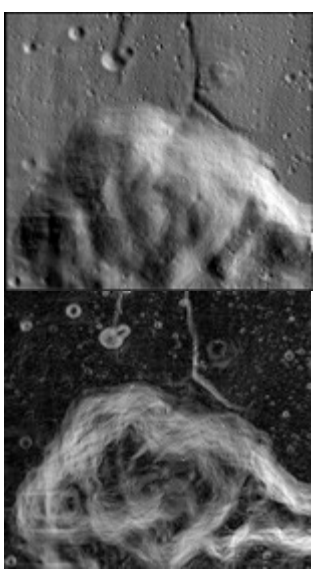

*Figure 1. Image of the incidence angle (top) and emission angle (bottom) for the region of study within Tsiolkovsky crater.*

**Stereophotoclinometry:** Using Lunar Reconnaissance Orbiter Camera (LROC) data, we constructed a digital elevation model (DEM) for a region within Tsiolkovsky crater using the techniques of sterophotoclinometry [6]. The selected region contains several types of terrains and a variety of slopes and slope orientations, including south-facing slopes that will have lower temperatures due to their lower insolation. The selected region includes mare floor materials, a rill within the mare, and an andesitic uplift from the central peak [7]. The source LROC data has a resolution of 0.5 meters, while the SPC generated DEM has a grid spaceing of 1.5 meters with a vertical precision of ~1 meter. From the DEM images of illumination (incidence angle) and viewing (emission angle) geometris can be constructed (Fig.1).

**Photometric Analysis:** Photometric cubes (layered images in which each layer contains specific data relevant to the pixel position within the cube) were constructed from each LROC image that fell within our region [7]. We generated a 4-band cube where the four layers contain the reflectance (I/F), phase angle (α), incidence angle (i), and emission angle (e). The I/F values come directly from the calibrated LRO NAC images. The phase angle is generated from the United States Geologic Survey (USGS) Integrated Software for Imagers and Spectrometers (ISIS) tool. Incidence and emission angles are calculated directly from the topographic SPC model using the spacecraft and sun positions. The NAC images are narrower than our region, so multiple images are required to fully mosaic the selected area.

The key component to generating the photometric cubes is the registration process performed by SPC. We use SPC to identify several thousand control-points (a.k.a. landmarks) in an image that locks its position to the existing DEM and registers it at one pixel accuracy. Once this is performed on all the images, any location within the working region (2,000 x 2,000 pixel) can be selected and the exact I/F for each observation of that surface feature, along with the associated α, i, and e can be retrieved. The data within the photometric cubes were modeled using Hapke's set of equations [8 – 14], where 10 x 10 pixel areas within the cubes defined a single data set to be modeled. The results are image cubes where the layers correspond to the parameter values for each parameter in the Hapke model (Fig. 2).

**Thermal Spectrum:** The next step in the analysis was the derivation of the thermal parameters in support of a thermal model. We calculated the geometric albedo, phase integral, and Bond albedo images using the Hapke parameters at each location (Fig. 3).

We generate a thermal sepectrum for every pixel using the insolution, the Bond albedo, an average emissivity of 0.9 and the incidence angle. The high

resolution DEM provides unparalleled detail of the surfaces' thermal model, allowing support for hot spots and shadows underfilling pixels.

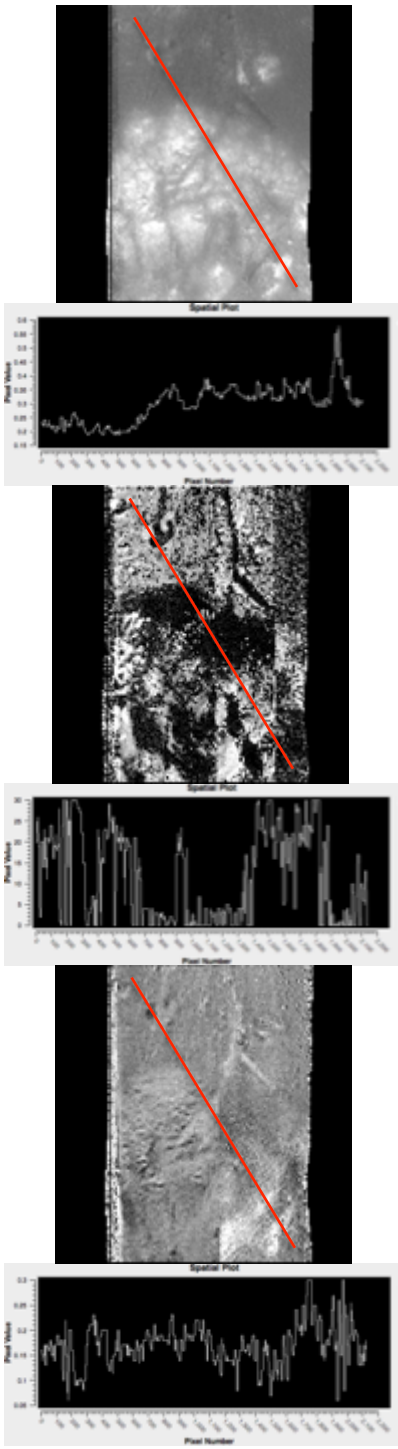

*Figure 2. Images of the Hapke model parameters corresponding to their physical location on the surface of our sample area within Tsiolkovsky carter. Top displays the single scattering albedo, center displays the surface roughness, and bottom displays the phase function parameter. Values along the red line are plotted from top-left to bottom-right along the scan.*

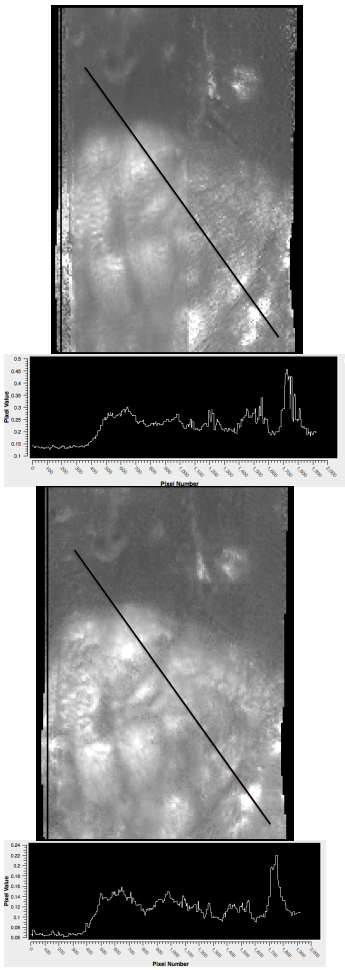

*Figure 3. Images of the geometric (top) and Bond (bottom) albedo values within the study area. Values along the black scan line are plotted below the image from top-left to bottom-right along the scan.*

**References:** [1] Vilas, F. et al. 2008. Earth Planets Space 60, 67. [2] Clark, R.N., 2009. Science 326, 562. [3] Pieters, C. M., et al. 2009. Science 326, 568. [4] Sunshine, J. M., et al. 2009. Science 326, 565. [5] Hendirx et al. 2016. 47th LPSC, 2857. [6] Gaskell R. W. (2008) Meteoritics & Planet. Sci. 43, 1049-1062. [7] Pieters, C.M. and S. Tompkins, JGR 104, 21935 – 21949. [8] Hapke, B., 1981. J. Geophys. Res. 68, 4571–4586. [9] Hapke, B., 1984. Icarus 59, 41–59. [10] Hapke, B., 1986. Icarus 67, 264–280. [11] Hapke, B., 1993. Theory of Reflectance and Emittance Spectroscopy. Cambridge University Press, N.Y., 455 pp. [12] Hapke, B., 2002. Icarus 157, 523–534. [13] Hapke, B., 2008. Icarus 195, 918–926. [14] Hapke, B., 2012. Theory of Reflectance and Emittance Spectroscopy. Cambridge University Press, N.Y., 2nd Ed., 513 pp.